The Cryosphere Discuss., 7, 1313–1358, 2013
www.the-cryosphere-discuss.net/7/1313/2013/
doi:10.5194/tcd-7-1313-2013
© Author(s) 2013. CC Attribution 3.0 License.

The Cryosphere Discussions
Open Access

This discussion paper is/has been under review for the journal The Cryosphere (TC).
Please refer to the corresponding final paper in TC if available.

Recent extreme light sea ice years in the Canadian Arctic Archipelago: 2011 and 2012 eclipse 1998 and 2007

S. E. L. Howell[1], T. Wohlleben[2], A. Komarov[3,4], L. Pizzolato[5], and C. Derksen[1]

[1]Climate Research Division, Environment Canada, Toronto, Canada
[2]Canadian Ice Service, Environment Canada, Ottawa, Canada
[3]Department of Electrical and Computer Engineering, University of Manitoba, Winnipeg, Canada
[4]Centre for Earth Observation Science, University of Manitoba, Winnipeg, Canada
[5]Department of Geography and Environmental Management, University of Waterloo, Waterloo, Canada

Received: 20 February 2013 – Accepted: 14 March 2013 – Published: 28 March 2013

Correspondence to: S. E. L. Howell (stephen.howell@ec.gc.ca)

Published by Copernicus Publications on behalf of the European Geosciences Union.

CC BY

Abstract

Record low mean September sea ice area in the Canadian Arctic Archipelago (CAA) was observed in 2011 (146×10^3 km^2), a level that was nearly exceeded in 2012 (150×10^3 km^2). These values eclipsed previous September records set in 1998 (200×10^3 km^2) and 2007 (220×10^3 km^2) and are ~ 60 % lower than the 1981–2010 mean September climatology. In this study, the driving processes contributing to the extreme light years of 2011 and 2012 were investigated, compared to previous extreme minima of 1998 and 2007, and contrasted against historic summer seasons with above average September ice area. The 2011 minimum was driven by positive July surface air temperature (SAT) anomalies that facilitated rapid melt, coupled with atmospheric circulation in July and August that restricted multi-year ice (MYI) inflow from the Arctic Ocean into the CAA. The 2012 minimum was also driven by positive July SAT anomalies (with coincident rapid melt) but further ice decline was temporarily mitigated by atmospheric circulation in August and September which drove Arctic Ocean MYI inflow into the CAA. Atmospheric circulation was comparable between 2011 and 1998 (impeding Arctic Ocean MYI inflow) and 2012 and 2007 (inducing Arctic Ocean MYI inflow). However, evidence of both preconditioned thinner Arctic Ocean MYI flowing into CAA and maximum landfast first-year ice (FYI) thickness within the CAA was more apparent leading up to 2011 and 2012 than 1998 and 2007. The rapid melt process in 2011 and 2012 was more intense than observed in 1998 and 2007 because of the thinner ice cover being more susceptible to positive SAT forcing. The thinner sea ice cover within the CAA in recent years has also helped counteract the processes that facilitate extreme heavy ice years. The recent extreme light years within the CAA are associated with a longer navigation season within the Northwest Passage.

Discussion Paper | Discussion Paper | Discussion Paper | Discussion Paper |

TCD

7, 1313–1358, 2013

Recent extreme light sea ice years in the Canadian Arctic Archipelago

S. E. L. Howell et al.

1 Introduction

Prior to the Arctic melt season of 2012, perhaps the most striking Arctic sea ice event in the passive microwave satellite era since 1979 was when the mean September Arctic sea ice extent and area fell to record lows of $4.3 \times 10^6\,km^2$ and $2.78 \times 10^6\,km^2$, respectively (NASATeam; Cavalieri et al., 1996), in 2007 (Stroeve et al., 2008). This dramatic loss of ice during 2007 was linked to anomalously high sea level pressure (SLP) over Beaufort Sea and Canadian Basin and anomalously low SLP over eastern Siberia that transported ice out of the Arctic (Ogi et al., 2008; Wang et al., 2009) together with high surface air temperature (SAT) over the central Arctic (Comiso et al., 2008) and the increased bottom melt of sea ice (Perovich et al., 2008). Years of gradual thinning of the Arctic sea ice made it susceptible to the 2007 anomalous forcing events (Maslanik et al., 2007; Lindsay et al., 2009); over the past three decades the Arctic Ocean's thick multi-year ice (MYI) has been gradually replaced with thinner first-year ice (FYI) (Maslanik et al., 2011). In 2012, mean September sea ice extent and area fell to $3.61 \times 10^6\,km^2$ and $2.11 \times 10^6\,km^2$, respectively (NASATeam; Cavalieri et al., 1996), shattering the previous 2007 record. The 2012 September mean value represents ~ 50 % less sea ice area within the Arctic compared to the 1981–2010 mean September climatology. 2012 sea ice conditions actually fell below the 2007 record in August, following a dramatic storm that tracked across the Arctic from Siberia and into the Canadian Arctic Archipelago (CAA) (Simmonds and Rudeva, 2012). Although the contributing processes behind the 2012 pan-Arctic ice loss have yet to be fully investigated, Zhang et al. (2013) found that the 2012 record low would have still occurred without the storm. The latter result is consistent with the view that Arctic's sea ice is now thinner and more vulnerable to anomalous atmospheric forcing compared to previous decades (Stroeve et al., 2011a).

To date, the record lightest sea ice year within the CAA was 2011 with a mean September area of $146 \times 10^3\,km^2$, but 2012 was a close second at $150 \times 10^3\,km^2$ (Fig. 1a–c). These values represent ~ 60 % less sea ice area within the CAA com-

TCD
7, 1313–1358, 2013

CC BY

pared to the 1981–2010 mean September climatology. Prior to 2011, the lightest ice year within the CAA occurred in 1998 with mean a September ice area of 200×10^3 km^2 and 2007 ranked as second lightest with mean September ice area of 220×10^3 km^2 (Fig. 1b, c). Interestingly, the driving processes behind the 1998 and 2007 minima were very different. As described in Howell et al. (2010), atmospheric circulation during the summer months of 1998 allowed predominantly warm southerly air masses to flow over the CAA. The resultant anomalously warm SAT and restriction of Arctic Ocean MYI inflow into the CAA combined to gradually ablate the thicker MYI over a longer than normal melt season. In 2007, anomalously warm July SAT facilitated an intense and rapid melt which led to light ice conditions in the CAA, but this was partially mitigated by high SLP over the Beaufort Sea which facilitated the inflow of Arctic Ocean MYI into the CAA. This Arctic Ocean ice inflow prevented 2007 from eclipsing the 1998 record. Furthermore, unlike 2007, sea ice in 1998 exhibited no evidence of preconditioned thinning leading up the minimum (Howell et al., 2010).

In the years that followed the record light ice year of 1998, the CAA returned to heavier summer ice conditions but the years that followed 2007 only witnessed a slight increase in end-of-summer ice (apparent in 2008 and 2009; Fig. 1c). Perhaps more striking is that 5 of the lightest ice years in the CAA since 1968 (i.e. 2007, 2008, 2010, 2011 and 2012) have all occurred within the last 6 yr (Fig. 1c). Considering the recent observed extreme light ice years within the CAA three questions need to be addressed: (i) what were the processes that contributed to the record extreme light ice years of 2011 and 2012?; (ii) how were these processes similar to or different from 1998 and 2007?; and (iii) what is the likelihood that the CAA will experience a heavy summer ice cover in upcoming years?

In order to answer these questions, this paper investigates the driving processes contributing to the extreme light years of 2011 and 2012, compares them to those responsible for the previous extreme minima of 1998 and 2007, and contrasts the processes behind extreme light sea ice years with those behind extreme heavy ice years. Understanding the driving processes behind light and heavy summer sea ice conditions

CC BY

within the CAA is important because when global climate models indicate a seasonally sea ice-free Arctic Ocean (i.e. less than 1 million km^2) they still find sea ice to be present within the CAA (e.g. Holland et al., 2006; Sou and Flato, 2009; Wang and Overland, 2012). Even as climate model resolution continues to improve, resolving sea ice thermodynamic and dynamic processes within the narrow channels of the CAA will still remain difficult. Knowledge the driving factors behind of heavy and light sea ice conditions in the CAA is also of particular importance for Northwest Passage shipping activities (ACIA, 2004; AMSA, 2009).

This paper is organized as follows. Section 2 describes the data and methods used in the analysis. Section 3 defines the framework of the study by looking at the CAA's extreme light and heavy ice years within a historical time series. Section 4 describes the melt season evolution of sea ice cover in the CAA during extreme light and heavy ice years. Section 5 discusses the thermodynamic and dynamic processes during these two types of seasons. Section 6 discusses the role of preconditioned ice thinning on the recent extreme minima. Section 7 discusses the implications for navigating the Northwest Passage given the recent occurrence of more frequent extreme ice minima. Conclusions are presented in Sect. 8.

2 Data and methods

2.1 Canadian Ice Service Digital Archive

Weekly total, MYI, and FYI concentration (tenths) and area (km^2) were extracted from the Canadian Ice Service Digital Archive (CISDA) for 1968 to 2012, from June to October for the CAA domain shown in Fig. 1a. The CISDA is a compilation of Canadian Ice Service regional weekly ice charts that integrate all available real-time sea ice information from various satellite sensors, aerial reconnaissance, ship reports, operational model results and the expertise of experienced ice forecasters, spanning 1968 to present (Canadian Ice Service, 2007). The CISDA ice charts are topologically complete

TCD
7, 1313–1358, 2013
Recent extreme light sea ice years in the Canadian Arctic Archipelago
S. E. L. Howell et al.

CC BY

polygon ArcInfo Geographic Information System coverages and available online from the CIS (http://ice.ec.gc.ca/).

The CISDA is more accurate than Scanning Multichannel Microwave Radiometer (SMMR) and Special Sensor Microwave/Imager (SSM/I) passive microwave ice concentration retrievals during the melt season (Agnew and Howell, 2003). The CISDA contains a technological bias (related to advances in sensor technology and changes in regional focus due to the emergence of important shipping routes; Canadian Ice Service, 2007), but Tivy et al. (2011) performed an extensive evaluation of the CISDA and found no evidence of time-varying biases in the period since 1979. The main focus of this study is on processes during light versus heavy ice seasons, not the trends in ice area or concentration therefore, the impact of any technological and methodological changes will exert minimal influence on the results. CISDA monthly averages of total, MYI, and FYI area and concentration were calculated for the melt season months of June to September. The 1981–2010 period was chosen to represent the historical climatology and standardized anomalies for total, MYI, and FYI were calculated by dividing anomalies by the 1981–2010 climatological standard deviation.

The years of 1972, 1979, 1997 and 2004 were selected as the extreme heavy ice years to compare against the four extreme low years of 1998, 2007, 2011 and 2012. 1972 and 1979 rank as to the two years with heaviest September ice conditions since 1968. 1997 (5th heaviest; Fig. 1c) and 2004 (6th heaviest; Fig. 1c) were selected instead of 1978 (3rd heaviest; Fig. 1c) and 1986 (4th heaviest; Fig. 1c) because the source of the CAA's MYI changed from FYI aging to a combination of FYI aging and Arctic Ocean MYI inflow in 1995 (Howell et al., 2009). Selecting heavy ice years in both periods allows for a more representative investigation of the processes behind heavy ice years.

2.2 Canadian Arctic Archipelago–Arctic Ocean ice exchange

Ice exchange between the CAA and the Arctic Ocean during the months of May to September was estimated at the M'Clure Strait and the Queen Elizabeth Islands (QEI)

CC BY

gates (Fig. 1a). While ice exchange does occur between the Amundsen Gulf and the Arctic Ocean, the Amundsen Gulf becomes ice-free during the summer months and ice exchange provides a negligible source of CAA ice replenishment during the melt season (Kwok, 2006; Agnew et al., 2008; Howell et al., 2008; Canadian Ice Service, 2011).

Ice exchange was derived from sequential RADARSAT-1 or RADARSAT-2 synthetic aperture radar (SAR) imagery with a spatial resolution of $\sim 200\,\mathrm{m\,pixel^{-1}}$ using the Canadian Ice Service's Automated Ice Tracking System (CIS-ASITS). For extreme light and heavy years (only the 1997 and 2004 heavy years were within the RADARSAT period) the temporal resolution of the RADARSAT imagery was between 2–5 days. A detailed description of the sea ice motion tracking system can be found in (Wohlleben et al., 2013) and (Komarov and Barber, 2013). Here we briefly outline key elements of the ice tracking algorithm. The system operates with two sequential SAR images and derives a detailed map of ice displacements for the time interval separating the images. The algorithm captures both translational and rotational components of ice motion based on a combination of the phase- and cross-correlation matching techniques. To reduce the computation time several pyramid levels are generated from the original SAR images. At each resolution level various ice features (e.g. cracks, floes, ridges) suitable for tracking are automatically identified. First, the ice motion is derived at the lowest resolution level. Then at each consecutive resolution level the system is guided by the vectors found at the previous resolution level. To eliminate erroneous ice motion vectors the algorithm compares ice drift vectors derived from the forward pass (tracking from the first image to the second one) and the backward pass (tracking from the second image to the first one). The remaining vectors are further filtered by thresholding their cross-correlation coefficients. Finally, at each resolution level, a high, medium or low level of confidence is assigned to each ice drift vector according to the cross-correlation coefficient value. The accuracy of the algorithm was thoroughly examined based on the visual detection of similar ice features in sequential SAR images and ground truthed with ice tracking beacon data for various ice conditions. In Komarov

TCD
7, 1313–1358, 2013

and Barber (2013) a very good agreement between the SAR derived vectors and the trajectories of drifting ice beacons located in close proximity (less than 3 km) to the nearest SAR ice motion vectors was observed. The root mean square error (RMSE) was 0.43 km for 36 comparison points.

Sea ice area flux was estimated using an approach similar to Kwok (2006) and Agnew et al. (2008). Sea ice motion for each image pair was first interpolated to each exchange gate including a buffer region of ~30 km on each side of the gate and then sampled at 5 km intervals across the gate. Sea ice area flux (F) at each gate was calculated using:

$$F = \sum c_i u_i \Delta x \quad (1)$$

where, Δx is the spacing along the gate (5 km), u_i is the ice motion normal to the flux gate at the ith location and c_i is the sea ice concentration obtained from the CISDA. Assuming the errors of the motion samples are additive, unbiased, uncorrelated and normally distributed, the uncertainty in area flux across the gates (σ_f) can estimated using:

$$\sigma_f = \sigma_e L / \sqrt{N_s} \quad (2)$$

where, $\sigma_e \sim 0.43\,\text{km}\,\text{day}^{-1}$ is the error in SAR derived ice velocities deduced from Komarov and Barber (2013), L is the width of the gate (km) and N_s is the number of samples across the gate. For the M'Clure Strait and QEI gates, the area flux uncertainty is ~12–14 $\text{km}^2\,\text{day}^{-1}$. For each exchange gate, sea ice flux estimates from all available image pairs were summed over each month for May to September.

2.3 Ice thickness

To investigated changes in CAA FYI thickness, maximum landfast ice thickness values from 1968–2012 were obtained from the Canadian Ice Thickness program that contains ice thickness measurements at a number of sites located throughout the CAA.

TCD
7, 1313–1358, 2013

Cambridge Bay, Resolute Bay, Eureka and Alert (see Fig. 1) were selected in order to represent thickness values ranging for the low to high latitudes regions of the CAA. These sites are located in shallow waters in bays and inlets where the oceanic heat flux has a negligible influence on ice growth and as a result, ice growth is almost entirely driven by atmospheric thermodynamic forcing (Brown and Cote, 1992; Dumas et al., 2006). Maximum thickness measurements were not available in 2001 for all sites and were not available for 2002 and 2003 at Cambridge Bay. Ice thickness measurements are taken at approximately the same location every year on a weekly basis at a location close to shore over a depth of water that exceeds maximum ice thickness (MANICE, 2005). Small changes in measurement location are acknowledged as a potential source of error.

The nonparametric Mann–Kendall test for randomness against trend (Mann, 1945; Kendall, 1955) was used to calculate the trend in maximum landfast ice thickness from 1968–2012 at the selected sites within the CAA. The slope of each trend was calculated using a Kendall's tau following an approach by Sen (1968). Prior to assessing trend statistical significance, each time series was pre-whitened to remove lag one autocorrelation using an approach described by Wang and Swail (2001).

Ice, Cloud, and land Elevation Satellite (ICESat) and IceBridge ice thickness estimates were obtained prior the melt season to investigate changes in the thickness of Arctic Ocean MYI that would flow into the CAA during the melt season. IceBridge thickness were provided the National Snow and Ice Data Center (Kurtz et al., 2012a) using the retrieval methodology described by Kurtz et al. (2012b). The ICESat ice thickness estimates are the same used in Kwok et al. (2009) and a full description of the retrieval methodology can be found in Kwok et al. (2007) and Kwok et al. (2008). For each year from 2009–2011, we selected the closest IceBridge flight line to the north of the CAA. These three flight lines covered the spatial domain in blue shown in Fig. 1a. The mean ICESat thickness for the same region was extracted from 2004–2008. The dates of the IceBridge flight lines and the ICESat time period is shown in Table 1.

TCD
7, 1313–1358, 2013

CC BY

2.4 Ancillary datasets

The date of melt onset and freeze onset from 1979–2012 within the CAA (Fig. 1a) was retrieved from the satellite passive microwave algorithm described by Markus et al. (2009). SLP and SAT data from 1968–2012 were also extracted from National Center for Environmental Prediction–National Center for Atmospheric Research (NCEP–NCAR) Reanalysis (Kalnay et al., 1996; Kistler et al., 2001).

3 Extreme light and heavy ice years within the historical context

A summary of standardized ice cover anomalies for the extreme light and heavy ice years is shown in Table 2. The monthly time series of June to September total ice and MYI area within the CAA is shown in Fig. 2. At the beginning of the melt season for the record light ice year of 2011, June total ice anomalies were only slightly negative (−0.27) while for second lowest ice year of 2012 they were positive at 0.99. These 2011 June anomalies were both weaker than those of the previous low years of 1998 (−2.12) and 2007 (−0.6). The total ice standardized anomaly for July 2011 of −2.62 was stronger than the July 1998 (−1.6), 2007 (−1.46) and 2012 (−1.32) anomalies. The August total ice anomaly of −3.27 for 2011 was considerably less than 1998 (−0.94) and 2007 (−2.03). The August 2012 total ice anomaly of −2.66 was also stronger than those of both 1998 and 2007. September total ice anomalies for 2011 (−2.42) and 2012 (−2.38) were both substantially stronger than those of 1998 (−1.85) and 2007 (−1.64). Not surprisingly, the heavy ice years tended to experience mostly positive total ice standardized anomalies for June and July. Total ice anomalies for heavy ice years during August and September were all positive.

The spatial distribution of mean June and September total ice and MYI for the light ice years is shown in Fig. 3 and for heavy ice years in Fig. 4. In June, negative total ice concentration anomalies for light years were located in peripheral regions of the CAA (e.g. Amundsen Gulf, M'Clure Strait and Lancaster Sound where melt had

CC BY

already begun). Negative MYI concentration anomalies in June were more widespread throughout the CAA (with the exception of positive MYI anomalies across the southern CAA in 1998; see Table 2) especially in 2012. June MYI concentrations for the extreme heavy ice years exhibited positive anomalies throughout most of the CAA.

In September, negative total ice concentration anomalies extended over most of the CAA for all extreme light years. The negative total ice anomalies were particularly strong and widespread in 2011 and 2012. The spatial location of negative total ice concentration anomalies for all light ice years was fairly similar, located primarily within the Western Parry Channel and M'Clintock Channel. The 2 channels were almost 100 % ice covered during the heavy ice years which may suggest these regions are more sensitive to anomalous thermodynamic atmospheric forcing events which produce light ice years. The light ice years contained virtually no strong positive MYI concentration anomalies in September. For heavy ice years, only 1972 experienced negative MYI concentration anomalies in the Western Parry Channel and M'Clintock Channel. With no coincident total ice concentration negative anomalies evident during that year, this suggests that FYI survived the melt season in these regions, a conclusion further supported by 1972 having the highest mean September FYI area on record (298×10^3 km^2; Fig. 2d)

Over the 45-yr record of sea ice conditions within the CAA, 2011 and 2012 both standout as extreme light ice years, even more so than 1998 and 2007, in which the previous record minima were observed. When compared to heavier ice years, a key characteristic of the light ice years was the increased presence of FYI, and the decreased presence of MYI, at the start of the melt season in June (except for 1998 – Table 2; Fig. 2a). Regionally, this was particularly apparent within the Western Parry Channel and M'Clintock Channel (Fig. 3). Although FYI melts more easily, which in turn is more likely facilitate light ice conditions under anomalous atmospheric forcing, it is important to note that the earlier breakup of thinner FYI increases the opportunity of MYI inflow from the Arctic Ocean. This process was shown to reduce total ice loss over the melt season (Howell et al., 2008, 2009). In order to investigate the driving

CC BY

processes that contributed to the new record low years of 2011 and 2012, and comment on the processes required for the CAA to experience a heavy ice year, we first investigate the melt seasonal sea ice area progression during both light and heavy ice years.

4 Melt season progression of Canadian Arctic Archipelago sea ice cover

4.1 Light years

The time series of weekly total ice, MYI and FYI for the extreme light ice years of 1998, 2007, 2011 and 2012 is shown in Fig. 5. Total ice for the record low year of 2011 initially tracked higher than that of the previous record low year of 1998 until early July when the rate of ice loss increased and eventually reached a record minimum of 97×10^3 km^2 on 5 September. The 2011 minimum was considerably lower than observed in 1998 (133×10^3 km^2 during the week of 28 September) and 2007 (175×10^3 km^2 during the week of 10 September). Total ice for 2012 tracked above previous extreme light years and the 1981–2010 climatological mean until mid-July when it experienced a very rapid rate of decline and reached the second lowest minimum in the observational record of 131×10^3 km^2 during the week of 10 September. Howell et al. (2010) characterized the 2007 ice loss as relatively rapid when compared against the gradual loss of 1998. However, the total ice time series in Fig. 5a shows that both 2011 and 2012 experienced an even more rapid rate of decline than 2007.

The time series of FYI (Fig. 5c) also highlights the gradual decline in 1998, the rapid decline in 2007 and even more rapid decline during 2011 and 2012. In addition, the FYI time series illustrates that virtually zero FYI remained following the melt season for all four extreme light ice years. The time series of MYI (Fig. 5b) indicates that both 1998 and 2011 exhibited almost no MYI increases during the melt season, indicating reduced inflow from the Arctic Ocean. 2007 and 2012 did, however, experience MYI

TCD
7, 1313–1358, 2013

CC BY

increases during August and September, indicating the inflow of MYI to the CAA from the Arctic Ocean.

In summary, in all four light ice seasons virtually all the FYI melted by the end of the summer. The rate of ice loss was relatively slow and persistent in 1998, while the rapid rate of decline in 2007 was exceeded in 2011 and 2012. MYI increases due to import from the Arctic Ocean mitigated the melt season ice loss in 2007 and 2012, while the lack of MYI import during the 1998 and 2011 melt seasons contributed to the record low ice minima set during those seasons.

4.2 Heavy years

The weekly time series of total ice, MYI and FYI for 1972, 1979, 1997 and 2004 are shown in Fig. 6. Both 1972 and 1979 exhibited a similar slow rate of total ice decline, reaching minima of 533×10^3 km^2 on 28 August and 535×10^3 km^2 on 6 September, respectively. 1997 and 2004 experienced a greater rate of decline compared to 1972 and 1979 and reached minima of 426×10^3 km^2 on 28 August and 431×10^3 km^2 on 6 September, respectively. The extreme heavy ice year minima, on average, represent ~ 80 % more ice area compared to the record light minimum of 2011. Extreme heavy ice year minima also occurred 1–2 weeks earlier than the light ice years indicating a shortened melt season.

The FYI and MYI time series (Fig. 6b, c) for the heavy ice years highlight the two processes associated with heavier ice covered summers within the CAA: FYI aging and Arctic Ocean MYI import. 1 October is the date each year on which any FYI remaining at the end of the melt season is promoted to MYI (i.e. FYI aging). Although the rate of FYI loss during 1997 and 2004 was greater than in 1972 and 1979, it was still considerably less than the FYI loss during the extreme light years (Figs. 5c and 6c). All four heavy ice seasons show a rapid increase in MYI after 1 October, ranging from $\sim 75 \times 10^3$ km^2 for 1997 to $\sim 250 \times 10^3$ km^2 for 1972. The latter values provide an approximant estimate of the amount of FYI that has survived the melt season and that was promoted to MYI. This process was almost completely absent during the extreme

TCD
7, 1313–1358, 2013

cc BY

light ice years because of the lack of FYI at the end of the melt season (Fig. 5c). The role of MYI import during heavy ice years was evident by comparing 1972 and 1979 with 1997 and 2004. Although the increase in MYI on 1 October for 1997 and 2004 was small when compared to 1972 and 1979, there was also a net increase in MYI from 4 June to 24 September that can be attributed to Arctic Ocean inflow.

In summary, 1972 and 1979 experienced a large end-of-season MYI increase from FYI aging, while both 1997 and 2004 experienced a MYI increase from a combination of FYI aging and Arctic Ocean MYI inflow. In order to explain these differences in the seasonal evolution of summer ice cover for both light and heavy years we now look at the driving thermodynamic and dynamic processes.

5 Thermodynamic and dynamic processes behind extreme ice years

5.1 Light years

The time series of mean June through September (JJAS) SAT anomalies shows positive departures for all extreme light years, with the 2012 anomaly of 2.28 °C exceeding the previous record high set in 1998 (Fig. 7). 1998 has long been recognized as one of the warmest years in the Canadian Arctic, which exerted a strong influence on CAA sea ice conditions along with other elements of the Canadian cryosphere (e.g. Jeffers et al., Alt et al., 2006; Atkinson et al., 2006; Howell et al., 2010). The mean JJAS SAT anomaly for the record low ice year of 2011 ranked third at 1.80 °C, while 2007 was the "coolest" of the extreme light years with an anomaly of 0.71 °C (Fig. 7). The weaker mean JJAS SAT anomaly of 2007 is a reflection of cooler monthly mean SAT from June to September compared to 1998, 2011 and 2012 (Fig. 8). For 2011 and 2012, positive SAT anomalies in July (Fig. 8a, b) contributed to rapid melt observed in these years. When compared to 2007 that also experienced rapid melt, the 2011 and 2012 July SAT anomalies were stronger (Fig. 8a–c). When compared to 1998, both 2011 and 2012 experienced similar positive SAT anomalies sustained from June to September

CC BY

(Fig. 8a, b, d) but the rate of ice area decline in 1998 was gradual as oppose to rapid that is likely attributed to the increased presence of thick MYI (Fig. 5a, b).

The timing of melt onset is also another important factor to consider with respect to thermodynamic forcing on sea ice minima. Perovich et al. (2007) demonstrated the melt processes is enhanced from an earlier melt onset by increasing the energy available for melt during the melt season that exerts an influence on the minimum area reached over the season. This was the case in 1998 when the earlier melt onset (−6.6 days) resulted in more total ice loss early in the melt season and contributed to the gradual melt of MYI throughout a long melt season (Figs. 5a, b, 9). For 2007, melt onset was not anomalously early and total ice conditions in June were similar to the 1981–2010 climatology (Figs. 5a, 9), but warm SAT in July then resulted in rapid ice loss. Analogous to 2007, melt onset for 2011 and 2012 were also not anomalously early and total ice conditions remained near the 1981–2010 climatology in June (Figs. 5a, 9). However, once melt onset began in 2011 and 2012, the sea ice-albedo feedback served to intensify the strong positive July SAT anomalies and facilitated an even more rapid melt than 2007. Freeze onset dates for 2011 and 2012 were also not anomalous late providing more support for rapid melt driving ice loss in 2011 and 2012 (Fig. 9).

Investigation of the corresponding driving dynamic processes indicated that in addition to rapid melt, the extreme minimum of 2011 was also driven by July and August atmospheric circulation that restricted Arctic Ocean inflow. Ice area flux estimates for 2011 show almost net zero exchange between the Arctic Ocean and QEI gates from May to August and a large net inflow of $\sim 21 \times 10^3$ km^2 in September (Fig. 10a). Ice area flux estimates indicate almost zero net exchange across the M'Clure Strait gate from May to September for 2011 (Fig. 10b). The weekly MYI time series for 2011 exhibited a gradual decline from June until the first week of September which provides further evidence that very little Arctic Ocean ice exchange occurred (Fig. 5b). Positive June to August SLP anomalies over the central Arctic Ocean and Greenland in 2011 (Fig. 11b) contributed to reduced exchange between the Arctic Ocean and CAA leading up the minimum by facilitating stagnant ice motion within the CAA (Fig. 10b). Arctic

CC BY

Ocean ice import via the QEI in September 2011 was caused by a shift in atmospheric circulation that occurred in September (Fig. 11b). MYI for 2011 also began to increase the week after the minimum was reached (Fig. 5b). Similar to 2011, 1998 also experienced reduced Arctic Ocean ice inflow, although June to September SLP anomalies were different (cf. Fig. 11b, d) with atmospheric circulation driving more ice outflow from the CAA into the Arctic Ocean at both the M'Clure and QEI gates in September 1998 (Fig. 10).

With respect to sea ice dynamic forcing for 2012, the minimum was initially driven by rapid melt but this ice loss was mitigated by Arctic Ocean MYI inflow. The majority of this inflow occurred via the M'Clure Strait in August (Fig. 10b) with MYI during August also exhibiting increases (Fig. 5b). The ice inflow is likely associated with the anomalously low SLP that tracked across the Arctic Ocean and into the CAA (Simmonds and Rudeva, 2012). Following the August ice inflow event, almost zero net ice area flux occurred in September at the M'Clure Strait but a small net inflow occurred into the QEI (Fig. 10). These Arctic Ocean ice inflow events reduced the CAA's rate of total ice decline, preventing total ice conditions from eclipsing the 2011 record low. This driving dynamic process observed in 2012 was similar to 2007. Although June to September SLP anomalies were different between 2012 and 2007 (Fig. 11a, c) both atmospheric circulation patterns facilitated Arctic Ocean inflow into the CAA. It should be noted however that the 2012 Arctic Ocean ice influx into the M'Clure Strait was driven by 2 single SLP driving events in August (not shown) that are lost in the August monthly SLP average. The key difference between 2012 and 2007 was that despite the net Arctic Ocean ice inflow at the M'Clure Strait in August and at QEI in September for 2012, MYI conditions did not remain high through the remainder of the 2012 melt season (i.e. the imported MYI subsequently melted; Fig. 5b). Stronger positive August and September SAT anomalies in 2012 relative to 2007 may have resulted in the ablation of more MYI (Fig. 8a, c).

Ice amounts in the CAA for the new record low years of 2011 and 2012 were not driven by the same combination of thermodynamic and dynamic driving processes as

TCD
7, 1313–1358, 2013

CC BY

1998 or 2007 but instead shared processes related to both. While pronounced melt events, either rapid (i.e. 2007, 2011 and 2012) or of long duration (i.e. 1998) is a necessary condition for extreme low ice seasons within the CAA, dynamics also play an important role. Specifically, dynamics can enhance the extreme minima by restricting ice inflow (i.e. 1998 and 2011), amplify the extreme minima by facilitating ice outflow (i.e. 1998), or prevent record-breaking minima by facilitating ice inflow (e.g. 2007 and 2012).

5.2 Heavy years

The three processes that are associated with heavy ice years are short melt seasons, low mean JJAS SAT anomalies and Arctic Ocean MYI import. The time series of JJAS SAT anomalies indicates negative anomalies were present for all the extreme heavy ice years with 1972 experiencing the strongest negative anomaly of −2.63 °C (Fig. 7). Negative June to September mean SAT anomalies covered the CAA for almost all months of the extreme heavy ice years (Fig. 12). For 1972 and 1979, negative monthly SAT anomalies (Fig. 12c, d) contributed to more FYI survival as evident from the considerable jump in the MYI weekly time series on 1 October (Fig. 6b). Satellite derived melt and freeze onset were not available for 1972, but for 1979 melt onset occurred late and freeze onset early (i.e. short melt season) (Fig. 9.) that contributed to more FYI survival and heavier ice conditions at the end of the melt season. No direct estimates of Arctic Ocean-CAA ice exchange were available for 1972 and 1979 but the time series of MYI for these years shows very little change prior to the 1 October promotion of FYI suggesting negligible Arctic Ocean-CAA ice exchange (Fig. 6b). SLP anomalies during August and September for 1979 and during September of 1972 indicate atmospheric circulation which favored Arctic Ocean ice inflow into the CAA (Fig. 13c, d), but the actual ice area flux was negligible because the CAA was already heavily congested with ice throughout the season which prevented appreciable ice exchange (Fig. 4a, b).

For the heavy ice years of 1997 and 2004, JJAS SAT anomalies were slightly negative at −0.73 °C and −0.74 °C, respectively (Fig. 7). Melt onset anomalies for 1997 and

TCD
7, 1313–1358, 2013

CC BY

2004 yr were near normal at 2.7 days and 5.4 days (Fig. 9) and freeze onset anomalies for 2004 were also near normal (−1 days) but for 1997 they were considerably late at −10 days (Fig. 9). The weaker SAT anomalies in 1997 and 2004 (compared to 1972 and 1979; Fig. 12) allowed for more summer melt and decreased survival of the FYI. However, the greater areas of open water in these years facilitated Arctic Ocean MYI inflow which compensated for the slightly increased ice loss from melt. Arctic Ocean net inflow occurred at the M'Clure Strait during August and September in 1997 and 2004 and at the QEI September in 2004 (Fig. 14; no RADARSAT imagery available for the QEI in September 1997). August and September SLP anomalies are consistent with these import processes (Fig. 13a, b) and the weekly time series of MYI also illustrates a net increase in MYI prior to 1 October for both 1997 and 2004 (Fig. 6b). Therefore, heavy ice conditions in 1997 and 2004 were driven by a combination of thermodynamic (reduced FYI melt) and dynamic (increased MYI import) forcing.

The CAA's extreme heavy ice years were either driven by thermodynamics alone (delayed and less intense melt seasons 1972 and 1979) or in concert with dynamics (i.e. 1997 and 2004). There is interplay between thermodynamics and dynamics during heavy ice years, whereby some in situ melt of FYI creates conditions within the CAA which are receptive to atmospherically driven ice inflow from the Arctic Ocean due to some open water fraction. During light ice seasons, extreme ice minima are generally not the result of thermodynamics alone, but are also influenced by dynamic processes (i.e. MYI exchange between the Arctic Ocean and CAA).

6 Evidence of recent preconditioning thinning

Both 2011 and 2012 were able to eclipse the previous extreme light ice years of 1998 and 2007 because of a preconditioned thinner sea ice cover. Consider that since 1968, the CAA has always experienced a period of recovery following a light ice year with previous studies indicating the recovery process can take between 2 and 5 yr (e.g. Melling, 2002; Alt et al., 2006; Atkinson et al., 2006; Howell et al., 2008). For example,

TCD
7, 1313–1358, 2013

CC BY

following the extreme light ice year of 1998, mean September total ice gradually returned to heavier ice amounts (Figs. 1c, 2). However, following the extreme light year of 2007, there was only a brief and small period of recovery in 2008 and 2009, after which ice conditions began to decline again (Figs. 1c, 2). The June time series of FYI and MYI exhibit divergent trajectories from 1968 to 2012 (increasing FYI; decreasing MYI) indicating an increased proportion of FYI in the CAA at the start of the melt season (Fig. 2a). Both populations of FYI and MYI have experienced evidence of preconditioned ice thinning, particularly since 2007, making them more susceptible to anomalous atmospheric forcing.

Pre-melt season ICESat and IceBridge derived MYI thickness values just north of the CAA are presented in Table 1 and the corresponding anomaly time series is presented in Fig. 15. Ice thickness values in this region have clearly decreased following the 2007 melt season. Some recovery in 2009 and 2010 was apparent but values were still thinner by almost 1 m when compared to 2004–2007. Given these considerable reductions it is very likely that the Arctic Ocean MYI that has entered the CAA following 2007 has been thinner and become more vulnerable to positive summer SAT forcing compared to previous years. Prior to the melt season of 2011, which experienced record low conditions, Arctic Ocean MYI thickness values were almost 2 m less compared to 2004–2007 values. Additional evidence of preconditioned Arctic Ocean MYI thinning was also apparent in 2012 during which less Arctic Ocean MYI inflow into the CAA survived the melt season compared to 1997, 2004 and 2007. Atmospheric circulation in 2012 drove the inflow of MYI from the Canadian Basin into the CAA, but by the end of the melt season most of this MYI melted (Fig. 5b). In recent years large amounts of MYI circulating around the Canadian Basin to the Eurasian Arctic has been found to have melted out in the vicinity of the Beaufort Sea (Kwok and Cunningham, 2010; Stroeve et al., 2011b). Arctic Ocean MYI inflow also occurred during the extreme light year of 2007 but a larger amount of this inflow survived (Fig. 5b), suggesting Arctic Ocean MYI is now less resistant to in situ melt in the CAA because it has thinned over the last 4–5 yr (Fig. 15).

TCD
7, 1313–1358, 2013

CC BY

Evidence of thinner FYI is apparent from the decreasing trends in maximum landfast ice thickness within the CAA. Every location except Resolute Bay is experiencing statistically significant declines in maximum landfast ice thickness (Table 2). The decreases are equivalent to ~ 27 cm of ice thickness loss since 1968. We suggest that longer melt seasons within the CAA (Fig. 9; Howell et al., 2009) are resulting in the increased absorption of solar radiation and subsequently delaying fall freeze onset that in turn has reduced the length of time for FYI within the CAA to grow. This thermal inertia process has two implications for the processes driving extreme heavy and light years. First, a thinner FYI is more susceptible to rapid melt events. The melt seasons of 2011 and 2012 began with June FYI fractions making up 77 % and 88 % of the CAA's total ice component respectively making it more susceptible to positive SAT anomalies and the enhancement of ice melt (i.e. rapid melt) via the ice-albedo feedback. Moreover, the melt season lengths for 2011 and 2012 were not anomalously long (Fig. 9) providing additional support that rapid ice loss in July from anomalously warm SAT was made possible because of a thinner ice cover. Second, FYI thickness in some regions of the CAA has likely decreased to a point where it can no longer survive the melt season and age to MYI. This is an important driving process behind extreme heavy years and its absence in recent years has also has likely played a role in the increased presence of FYI at the start of the melt season (Fig. 2a). Polyakov et al. (2012) suggest the process of thermal inertia may be responsible for reduced MYI replenishment in certain regions of the Arctic Ocean. Dumas et al. (2006) also attributed projected declines in CAA landfast ice thickness to thermal inertia.

It seems apparent that in both 2011 and 2012 the MYI flowing into the CAA and the FYI within the CAA was preconditioned to be susceptible to anomalous forcing, which resulted in extreme minima, even more so than in 1998 and 2007. It is however important to note that the lack of preconditioned ice thinning in the CAA does not always prevent record light years. For example, the ice in 1998 exhibited no evidence of preconditioning yet an extreme minimum was still reached (Howell et al., 2010). Conversely, evidence of preconditioned thinning does not always prevent a heavy ice

TCD
7, 1313–1358, 2013

year from occurring. For example, because 1971 was a relatively light ice year, the 1972 melt season began with a low percentage of MYI within the CAA, and yet 1972 ended up being the heaviest ice year on record.

7 Implications for navigating the Northwest Passage

The extreme ice minima observed within CAA in recent years has resulted in increased open water within the CAA and in turn the Northwest Passage. The time series of length of the navigation season and mean MYI over the navigation season for northern route of the Northwest Passage is show in Fig. 16. The Canadian Ice Service defines the navigation season as "open" for any given week if the total ice extent within the route is less 60 % of the total ocean area within the route. There is a strong inverse correlation between the length of the navigation and mean MYI area present over shipping season of $r = -0.72$. The recent extreme light ice years within the CAA since 2007 are clearly associated with longer navigation seasons. The only other time period the northern route experienced a longer navigation season was from 1998–2000 that was also associated with the extreme sea ice minima (i.e. 1998).

Recent studies suggest that the northern route of the Northwest Passage is expected be a viable shipping route by mid-century (e.g. Smith and Stephenson, 2013; Stephenson et al., 2013). Based on observations there was certainly less MYI within the northern route over the shipping season in recent years (Fig. 16). However, MYI even in small concentrations is a serious hazard to transiting ships, and therefore caution should be taken with respect to the practical usage of the northern route in upcoming years. Specifically, the oldest and thickness MYI in the world lies on the north facing coast of the CAA and despite that fact that it has thinned in recent years (Fig. 15) it will continue to flow southward into the CAA and subsequently into the Northwest Passage (Melling, 2002; Howell et al., 2009). In addition, the coupling of preconditioned ice thinning, rapid melt and anomalous atmospheric circulation is responsible for clearing of the northern route, but clearing is only temporary as MYI returns to region from the QEI

CC BY

when predominant atmospheric circulation prevails (Howell et al., 2009). As a result, the presence of MYI is likely to remain within the northern route despite extreme light ice conditions and a longer navigation season. Given the projected pattern of Arctic Ocean ice retreat (e.g. Wang and Overland, 2012) transit across the Arctic Ocean will likely be more viable than through the northern route of Northwest Passage given the continued presence of MYI.

8 Conclusions

We began this paper by first asking the questions: *What were the processes that contributed to the new record extreme light ice years of 2011 and 2012 and how were they similar or different from 1998 and 2007?* The record low ice year of 2011 was driven by positive July SAT anomalies that facilitated rapid melt, together with July and August atmospheric circulation that restricted Arctic Ocean MYI inflow into the CAA. Although atmospheric circulation patterns between 1998 and 2011 were different, their resulting dynamic forcing on the sea ice was similar in that MYI inflow from the Arctic Ocean was impeded. The second lightest ice year of 2012 was also driven by positive July SAT anomalies that facilitated rapid melt, but August and September atmospheric circulation temporarily reduced the rapid rate of ice decline through MYI inflow from the Arctic Ocean. This positive ice area flux into the CAA prevented 2012 from surpassing the 2011 record. Of greater importance was the considerable evidence of preconditioned ice thinning prior 2011 and 2012 which made the sea ice more vulnerable to anomalous atmospheric forcing facilitating these extreme years.

The final question we posed was: *What is the likelihood that the CAA will experience a heavy summer ice cover in upcoming years?* Extreme heavy ice years in the CAA were found to be driven by (i) strongly negative SAT anomalies that reduced FYI decline over the melt season or (ii) moderate negative SAT anomalies that allowed slightly more ablation of FYI, but where MYI inflow from the Arctic Ocean compensated for the extra FYI loss. The CAA could experience a heavy ice year if either of these processes was

TCD
7, 1313–1358, 2013

CC BY

to occur again however, considerable evidence for a thinner seasonal ice cover within the CAA as well as Arctic Ocean MYI flowing into the CAA was apparent. A thinner ice cover (i.e. FYI and MYI) is less likely to survive the summer melt season and in turn counteracts the processes that facilitate extreme heavy ice years within the CAA. The CAA's lack of MYI recovery since 2007 (evidenced by 5 of the record lightest ice years all occurring within the last 6 yr) and the associated trends towards warmer Arctic SAT (Kaufman et al., 2009; Berkryaev et al., 2011) and a longer Arctic melt seasons (Howell et al., 2009; Markus et al., 2009) also serve to reduce the probability of the CAA experiencing an extreme heavy ice year in the near future. If light sea ice conditions within the CAA persist, so will longer navigation seasons with the northern route of the Northwest Passage but the presence of MYI will still remain.

Acknowledgements. This work was funded by the Canadian Space Agency through the Government Related Initiatives Program. We would like to thank T. Markus and J. Miller at Cryospheric Sciences Laboratory NASA GSFC for providing the SMMR-SSM/I melt and freeze onset data. RADARSAT data for 1997, 1998, 2004 and 2007 were provided by the Alaska Satellite Facility, Fairbanks, Alaska.

References

ACIA: Arctic Climate Impact Assessment, Cambridge University Press, Cambridge, 2004.

Agnew, T. and Howell, S.: The use of operational ice charts for evaluating passive microwave ice concentration data, Atmos. Ocean, 41, 317–331, doi:10.3137/ao.410405, 2003.

Agnew, T., Lambe, A., and Long, D.: Estimating sea ice area flux across the Canadian Arctic Archipelago using enhanced AMSR-E, J. Geophys. Res., 113, C10011, doi:10.1029/2007JC004582, 2008.

Alt, B., Wilson, K., and Carrieres, T.: A case study of old ice import and export through Peary and Sverdrup channels in the Canadian Arctic Archipelago: 1998–2004, Ann. Glaciol., 44, 329–338, doi:10.3189/172756406781811321, 2006.

AMSA: The Arctic Marine Shipping Assessment 2009 Report, Arctic Council, 2009.

TCD

7, 1313–1358, 2013

CC BY

Atkinson, D. E., Brown, R., Alt, B., Agnew, T., Bourgeois, J., Burgess, M., Duguay, C., Henry, G., Jeffers, S., Koerner, R., Lewkowicz, A. G., McCourt, S., Melling, H., Sharp, M., Smith, S., Walker, A., Wilson, K., Wolfe, S., Woo, M-k., and Young, K. L.: Canadian cryospheric response to an anomalous warm summer: a synthesis of the climate change action fund project "The State of the Arctic Cryosphere During the Extreme Warm Summer of 1998, Atmos. Ocean, 44, 347–375, doi:10.3137/ao.440403, 2006.
Berkryaev, R. V., Polyakov, I. V., and Alexeev, V. A.: Role of Polar amplification in long-term surface air temperature variations and modern Arctic warming, J. Climate, 23, 3888–3906, doi:10.1175/2010JCLI3297.1, 2011.
Brown, R. D. and Cote, P.: Interannual variability of landfast ice thickness in the canadian high Arctic, 1950–1989, Arctic, 45, 273–284, 1992.
Canadian Ice Service: Regional charts: history, accuracy, and caveats, Arch. Ser. Doc. Ser. 1, Ottawa, available at: http://ice.ec.gc.ca/IA_DOC/cisads_no_001_e.pdf, 2007.
Canadian Ice Service: Sea Ice Climatic Atlas: Northern Canadian Waters 1981–2010, edited by: Canadian Ice Service, Ottawa, Canada, 995 pp., 2011.
Cavalieri, D., Parkinson, C., Gloersen, P., and Zwally, H. J.: Sea Ice Concentrations from Nimbus-7 SMMR and DMSP SSM/I-SSMIS Passive Microwave Data, updated yearly, National Snow and Ice Data Center, Boulder, Colorado, USA, 1996.
Comiso, J. C., Parkinson, C. L., Gersten, R., and Stock, L.: Accelerated decline in the Arctic sea ice cover, Geophys. Res. Lett., 35, L01703, doi:10.1029/2007GL031972, 2008.
Dumas, J. A., Flato, G. M., and Brown, R. D.: Future projections of landfast ice thickness and duration in the Canadian Arctic, J. Climate, 19, 5175–5189, doi:10.1175/JCLI3889.1, 2006.
Jeffers, S., Agnew, T., Alt, B., De Abreu, R., and McCourt, S.: Investigating the anomalous sea-ice conditions in the Canadian High Arctic (Queen Elizabeth Islands) during summer 1998, Ann. Glaciol., 33, 507–512, 2001.
Howell, S. E. L., Tivy, A., Yackel, J. J., Else, B. G. T., and Duguay, C. R.: Changing sea ice melt parameters in the Canadian Arctic Archipelago: implications for the future presence of multiyear ice, J. Geophys. Res., 113, C09030, doi:10.1029/2008JC004730, 2008.
Howell, S. E. L., Duguay, C. R., and Markus, T.: Sea ice conditions and melt season duration variability within the Canadian Arctic Archipelago: 1979–2008, Geophys. Res. Lett., 36, L10502, doi:10.1029/2009GL037681, 2009.

TCD
7, 1313–1358, 2013

CC BY

Howell, S. E. L., Tivy, A., Agnew, T., Markus, T., and Derksen, C.: Extreme low sea ice years in the Canadian Arctic Archipelago: 1998 versus 2007, J. Geophys. Res., 115, C10053, doi:10.1029/2010JC006155, 2010.
Kalnay, E. and Coauthors: The NCEP/NCAR 40-yr reanalysis project, B. Am. Meteorol. Soc., 77, 437–471, 1996.
Kaufman, D. S., Schneider, D. P., McKay, N. P., Ammann, C. M., Bradley, R. S., Briffa, K. R., Miller, G. H., Otto-Bliesner, B. L., Overpeck, J. T., Vinther, B., and Arctic Lakes 2k Project Members: Recent warming reverses long-term Arctic cooling, Science, 325, 1236–1239, doi:10.1126/science.1173983, 2009.
Kendall, M. G.: Rank Correlation Methods, Charles Griffin, 196 pp., 1955.
Kistler, R. and Coauthors: The NCEP–NCAR 50-yr reanalysis: monthly means CD-ROM and documentation, B. Am. Meteorol. Soc., 82, 247–267, 2001.
Komarov, A. S. and Barber, D. G.: Sea ice motion tracking from sequential dual-polarization RADARSAT-2 images, IEEE T. Geosci. Remote, doi:10.1109/TGRS.2012.2236845, 2013.
Kwok, R.: Exchange of sea ice between the Arctic Ocean and the Canadian Arctic Archipelago, Geophys. Res. Lett., 33, L16501, doi:10.1029/2006GL027094, 2006.
Kwok, R. and Cunningham, G. F.: Contribution of melt in the Beaufort Sea to the decline in Arctic multiyear sea ice coverage: 1993–2009, Geophys. Res. Lett., 37, L20501, doi:10.1029/2010GL044678, 2010.
Kwok, R., Cunningham, G. F., Zwally, H. J., and Yi, D.: ICESat over Arctic sea ice: interpretation of altimetric and reflectivity profiles, J. Geophys. Res., 111, C06006, doi:10.1029/2005JC003175, 2006.
Kwok, R., Cunningham, G. F., Zwally, H. J., and Yi, D.: Ice, Cloud, and land Elevation Satellite (ICESat) over Arctic sea ice: retrieval of freeboard, J. Geophys. Res., 112, C12013, doi:10.1029/2006JC003978, 2007.
Kwok, R., Cunningham, G. F., Wensnahan, M., Rigor, I., Zwally, H. J., and Yi, D.: Thinning and volume loss of the Arctic Ocean sea ice cover: 2003–2008, J. Geophys. Res., 114, C07005, doi:10.1029/2009JC005312, 2009.
Kurtz, N., Studinger, M., Harbeck, J., Onana, V., Farrell, S.: IceBridge Sea Ice Freeboard, Snow Depth, and Thickness, NASA DAAC at the National Snow and Ice Data Center, Boulder, Colorado, USA, 2012a.
Kurtz, N. T., Farrell, S. L., Studinger, M., Galin, N., Harbeck, J. P., Lindsay, R., Onana, V. D., Panzer, B., and Sonntag, J. G.: Sea ice thickness, freeboard, and snow depth prod-

CC BY

ucts from Operation IceBridge airborne data, The Cryosphere Discuss., 6, 4771–4827, doi:10.5194/tcd-6-4771-2012, 2012b.
Lindsay, R. W., Zhang, J., Schweiger, A., Steele, M., and Stern, H.: Arctic sea ice retreat in 2007 follows thinning trend, J. Climate, 22, 165–176, doi:10.1175/2008JCLI2521.1, 2009.
MANICE: Manual of Standard Procedures for Observing and Reporting Ice Conditions, Canadian Ice Service, Meteorological Service of Canada, 146 pp., 2005.
Mann, H. B.: Non-parametric tests against trend, Econometrica, 13, 245–259, 1945.
Markus, T., Stroeve, J. C., and Miller, J.: Recent changes in Arctic sea ice melt onset, freezeup, and melt season length, J. Geophys. Res., 114, C12024, doi:10.1029/2009JC005436, 2009.
Maslanik, J. A., Fowler, C., Stroeve, J. C., Drobot, C., Zwally, J., Yi, D., and Emery, W.: A younger, thinner Arctic ice cover: Increased potential for rapid, extensive sea-ice loss, Geophys. Res. Lett., 34, L24501, doi:10.1029/2007GL032043, 2007.
Maslanik, J., Stroeve, J. C., Fowler, C., and Emery, W.: Distribution and trends in Arctic sea ice age through spring 2011, Geophys. Res. Lett., 38, L13502, doi:10.1029/2011GL047735, 2011.
Melling, H.: Sea ice of the northern Canadian Arctic Archipelago, J. Geophys. Res., 107, C113181, doi:10.1029/2001JC001102, 2002.
Ogi, M., Rigor, I. G., McPhee, M. G., and Wallace, J. M.: Summer retreat of Arctic sea ice: role of summer winds, Geophys. Res. Lett., 35, L24701, doi:10.1029/2008GL035672, 2008.
Perovich, D. K., Nghiem, S. V., Markus, T., and Schweiger, A.: Seasonal evolution and interannual variability of the local solar energy absorbed by the Arctic sea ice–ocean system, J. Geophys. Res., 112, C03005, doi:10.1029/2006JC003558, 2007.
Perovich, D. K., Richter-Menge, J. A., Jones, K. F., and Light, B.: Sunlight, water and ice: extreme Arctic sea ice melt during the summer of 2007, Geophys. Res. Lett., 35, L11501, doi:10.1029/2008GL034007, 2008.
Polyakov, I. V., Walsh, J. E., and Kwok, R.: Recent changes of Arctic multiyear sea ice coverage and the likely causes, B. Am. Meteorol. Soc., 145–151, doi:10.1175/BAMS-D-11-00070.1, 2012.
Sen, P. K.: Estimates of the regression coefficient based on Kendall's tau, J. Am. Stat. Assoc., 63, 1379–1389, doi:10.2307/2285891, 1968.
Simmonds, I. and Rudeva, I.: The great arctic cyclone of August 2012, Geophys. Res. Lett., 39, L23709, doi:10.1029/2012GL054259, 2012.

TCD
7, 1313–1358, 2013

CC BY

Sou, T. and Flato, G.: Sea ice in the Canadian Arctic Archipelago: modeling the past (1950–2004) and the future (2041–60), J. Climate, 22, 2181–2198, doi:10.1175/2008JCLI2335.1, 2009.

Stroeve, J., Serreze, M., Drobot, S., Gearheard, S., Holland, M., Maslanik, J., Meier, W., and Scambos, T.: Arctic sea ice extent plummets in 2007, Eos Trans. AGU, 89, 13–14, doi:10.1029/2008EO020001, 2008.

Stroeve, J., Serreze, M., Holland, M., Kay, J., Maslanik, J., and Barrett, A.: The Arctic's rapidly shrinking sea ice cover: a research synthesis, Climatic Change, 110, 1005–1027, doi:10.1007/s10584-011-0101-1, 2011a.

Stroeve, J. C., Maslanik, J., Serreze, M. C., Rigor, I., Meier, W., and Fowler, D.: Sea ice response to an extreme negative phase of the Arctic Oscillation during winter 2009/2010, Geophys. Res. Lett., 38, L02502, doi:10.1029/2010GL045662, 2011b.

Tivy, A., Howell, S. E. L., Alt, B., McCourt, S., Chagnon, R., Crocker, G., Carrieres, T., and Yackel, J. J.: Trends and variability in summer sea ice cover in the Canadian Arctic based on the Canadian Ice Service Digital Archive, 1960–2008 and 1968–2008, J. Geophys. Res., 116, C03007, doi:10.1029/2009JC005855, 2011.

Wang, J., Zhang, J., Watanabe, E., Ikeda, M., Mizobata, K., Walsh, J. E., Bai, X., and Wu, B.: Is the dipole anomaly a major drier to record lows in Arctic summer sea ice extent?, Geophys. Res. Lett., 36, L05706, doi:10.1029/2008GL036706, 2009.

Wang, M. and Overland, J. E.: A sea ice free summer Arctic within 30 years – an update from CMIP5 models, Geophys. Res. Lett., 39, L18501, doi:10.1029/2012GL052868, 2012.

Wang, X. L. and Swail, V. R.: Changes of extreme wave heights in Northern Hemisphere oceans and related atmospheric circulation regimes, J. Climate, 14, 2204–2221, doi:10.1175/1520-0442(2001)014<2204:COEWHI>2.0.CO;2, 2001.

Wohlleben, T., Howell, S. E. L., Agnew, T., and Komarov: Sea-ice motion and flux within the Prince Gustaf Adolf Sea, Queen Elizabeth Islands, Canada during 2010, Atmos.-Ocean, 51, 1–17, doi:10.1080/07055900.2012.750232, 2013.

Zhang, J., Lindsay, R., Schweiger, A., and Steele, M.: The impact of an intense summer cyclone on 2012 Arctic sea ice retreat, Geophys. Res. Lett, 40, doi:10.1002/grl.50190, 2013.

TCD
7, 1313–1358, 2013
Recent extreme light sea ice years in the Canadian Arctic Archipelago
S. E. L. Howell et al.

Table 1. ICESat and IceBridge ice thickness estimates within the Canadian Basin just north of the Canadian Arctic Archipelago, 2004–2011.

Year	Ice Thickness (m)	Sensor	Date
2004	5.6	ICESat	Feb–Mar
2005	5.6	ICESat	Feb–Mar
2006	5.1	ICESat	Feb–Mar
2007	5.2	ICESat	Apr–May
2008	3.3	ICESat	Feb–Mar
2009	3.9	IceBridge	21 Apr 2009
2010	4.4	IceBridge	5 Apr 2010
2011	3.7	IceBridge	16 Mar 2011

TCD
7, 1313–1358, 2013

Table 2. Monthly June to September total, multi-year ice (MYI) and first-year ice (FYI) standardized anomalies for extreme light and heavy sea ice years in the Canadian Arctic Archipelago. Standardized anomalies calculated with respect to the 1981–2010 climatology.

	Total	MYI	FYI	Total	MYI	FYI	Total	MYI	FYI	Total	MYI	FYI
		2012			2011			2007			1998	
Jun	0.99	−2.06	2.23	−0.27	−1.04	0.88	−0.6	−1.03	0.74	−2.12	1.08	−1.67
Jul	−1.32	−2.01	1.23	−2.62	−1.23	−0.30	−1.46	−0.98	−0.13	−1.6	1.04	−1.91
Aug	−2.66	−1.62	−1.47	−3.27	−1.95	−1.86	−2.03	−1.24	−1.06	−0.94	0.74	−1.87
Sep	−2.38	−2.25	−1.21	−2.42	−2.37	−1.52	−1.64	−1.15	−1.19	−1.85	−1.06	−1.20
		2004			1997			1979			1972	
Jun	0.46	0.34	−0.15	−0.08	0.98	−0.91	1.89	1.98	−1.15	0.28	0.90	−0.97
Jul	0.80	0.30	0.17	−0.04	1.00	−1.01	2.33	1.91	−0.54	1.98	0.08	1.03
Aug	0.97	0.53	0.59	0.56	1.02	−0.43	2.40	2.23	0.38	0.41	1.87	−1.50
Sep	1.55	1.21	0.88	1.58	1.63	0.18	2.29	2.13	1.10	2.58	−0.34	4.25

TCD
7, 1313–1358, 2013

CC BY

Table 3. Trends in maximum landfast ice thickness at selected sites within the Canadian Arctic Archipelago, 1968–2012. Also shown is the accumulated 43 yr ice loss.

Site	Sen's Slope	*p* value	43 yr ice loss (cm)
Alert	−0.66	0.03	28.8
Eureka	−0.55	0.03	23.8
Resolute Bay	−0.19	0.57	8.4
Cambridge Bay	−0.71	0.04	30.8

TCD
7, 1313–1358, 2013

CC BY

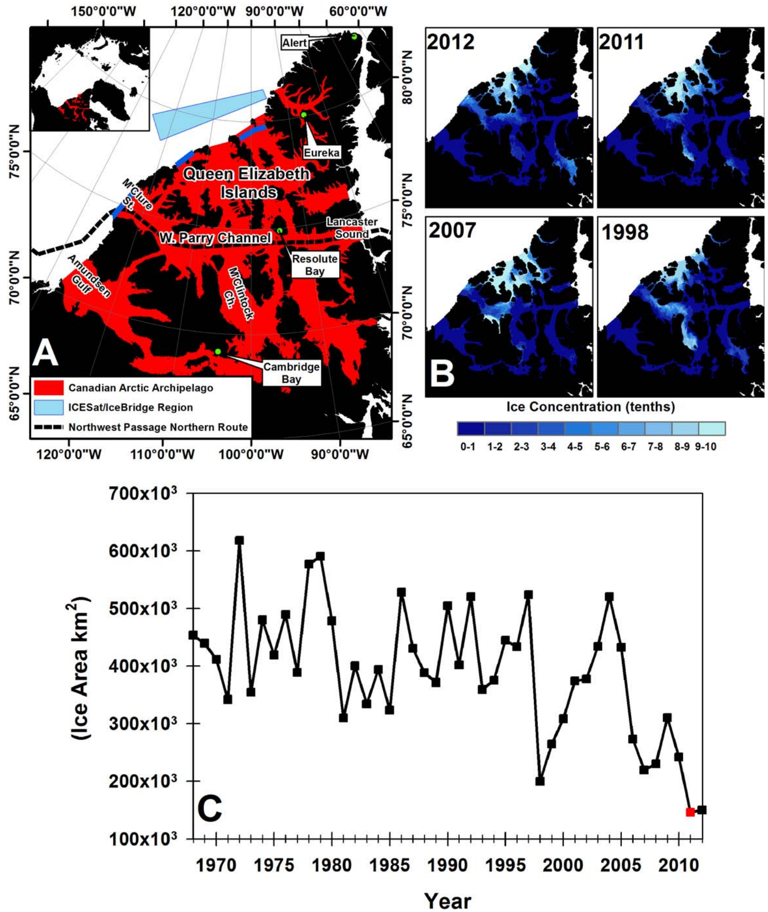

Fig. 1. The geographical location of the Canadian Arctic Archipelago (CAA) **(A)**, spatial distribution of CAA mean September total ice concentration (tenths) for the four extreme light years **(B)** and the time series of CAA mean September sea ice area (km^2), 1968–2012 **(C)**.

CC BY

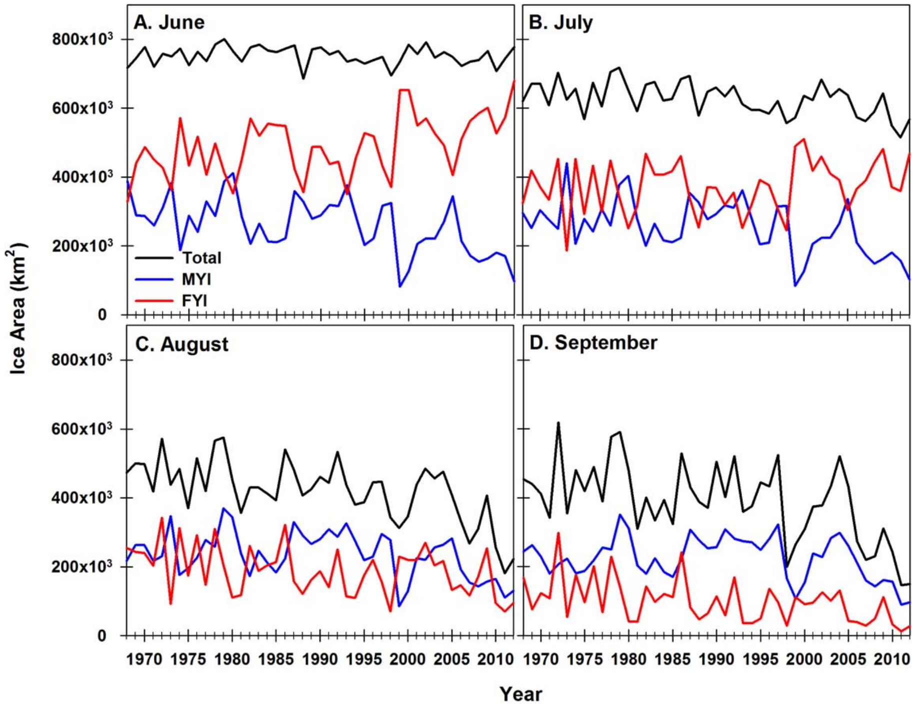

Fig. 2. Time series of mean monthly total ice, multi-year ice (MYI) and first-year ice (FYI) area (km^2) within the Canadian Arctic Archipelago for June to September **(A–D)** from 1968–2012.

TCD
7, 1313–1358, 2013

CC BY

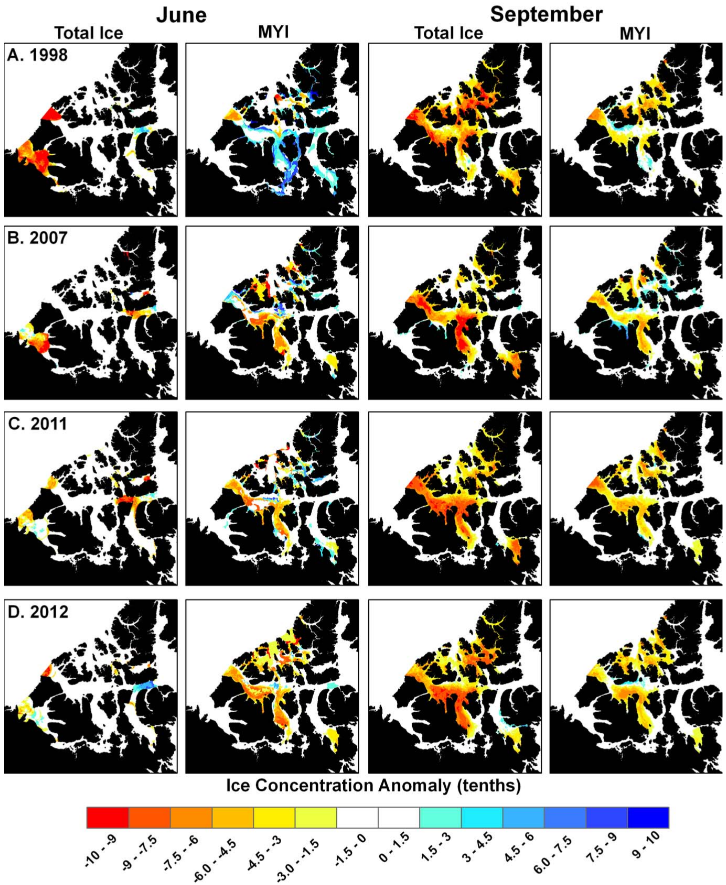

Fig. 3. Spatial distribution of June and September total ice and multi-year ice (MYI) concentration anomalies (tenths) for 2012, 2011, 2007 and 1998 within the Canadian Arctic Archipelago **(A–D)**. Anomalies calculated with respect to the 1981–2010 climatology.

TCD
7, 1313–1358, 2013

CC BY

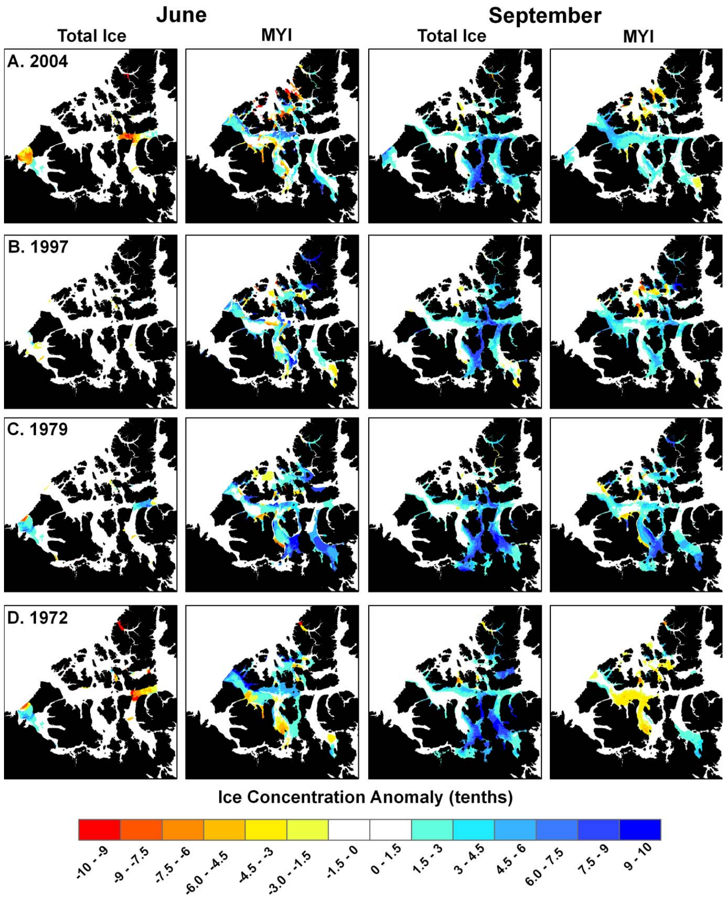

Fig. 4. Spatial distribution of June and September total ice and multi-year ice (MYI) concentration anomalies (tenths) for 2004, 1997, 1979 and 1972 within the Canadian Arctic Archipelago **(A–D)**. Anomalies calculated with respect to the 1981–2010 climatology.

CC BY

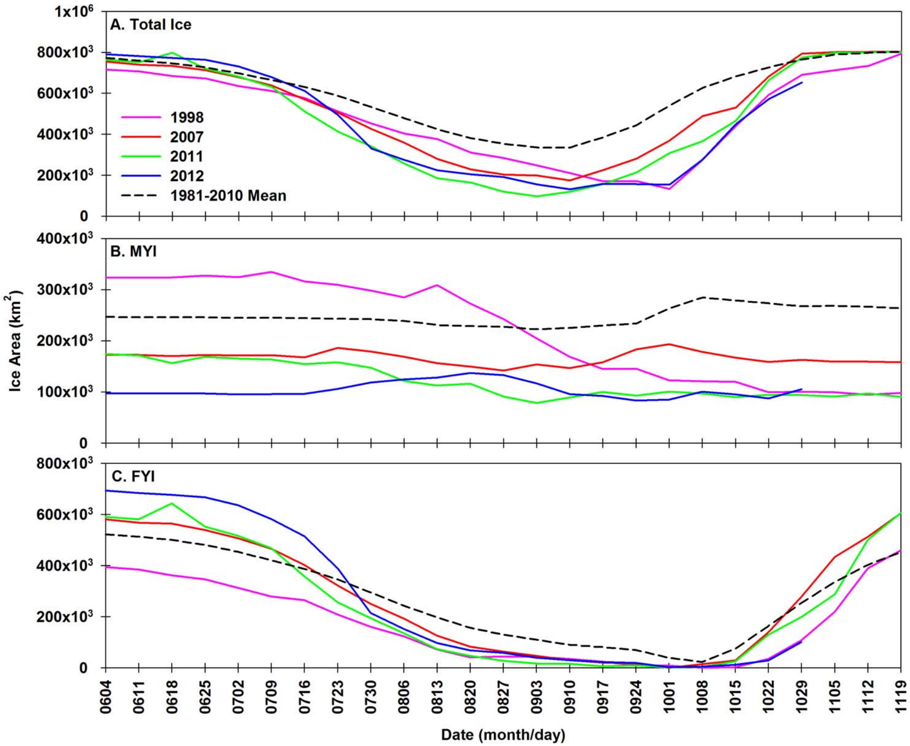

Fig. 5. Weekly time series of total ice **(A)**, multi-year (MYI) **(B)** and first year ice (FYI) **(C)** area (km^2) for 1998, 2007, 2011 and 2012 in the Canadian Arctic Archipelago.

TCD
7, 1313–1358, 2013

cc BY

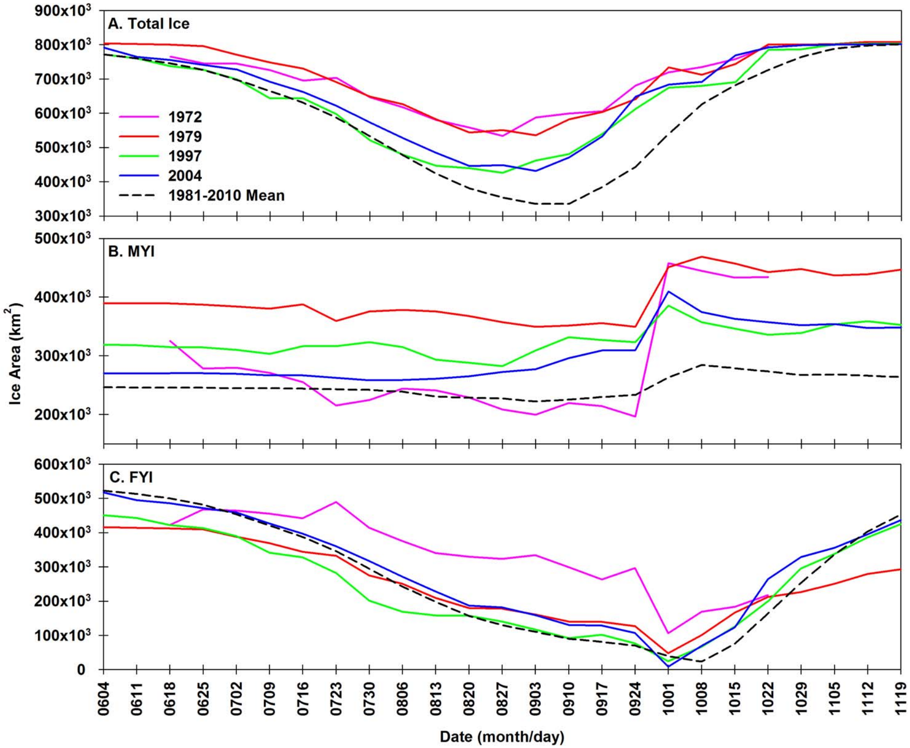

Fig. 6. Weekly time series of total ice **(A)**, multi-year (MYI) **(B)** and first year ice (FYI) **(C)** area (km^2) for 1972, 1979, 1997 and 2004 in the Canadian Arctic Archipelago.

CC BY

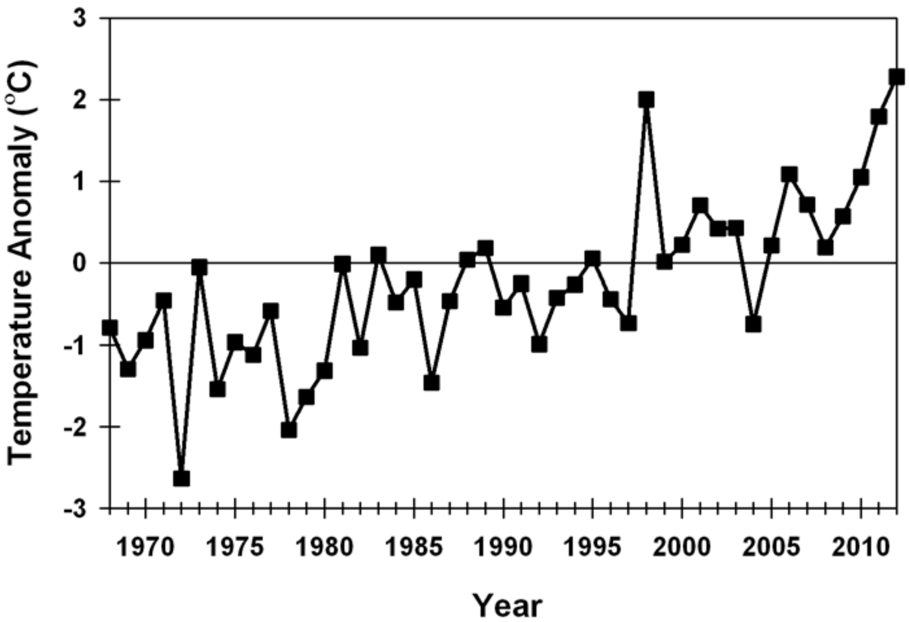

Fig. 7. Time series of the mean June through September (JJAS) surface air temperature (SAT) anomalies (°C) in the Canadian Arctic Archipelago, 1968–2012. Anomalies calculated with respect to the 1981–2010 climatology.

TCD
7, 1313–1358, 2013

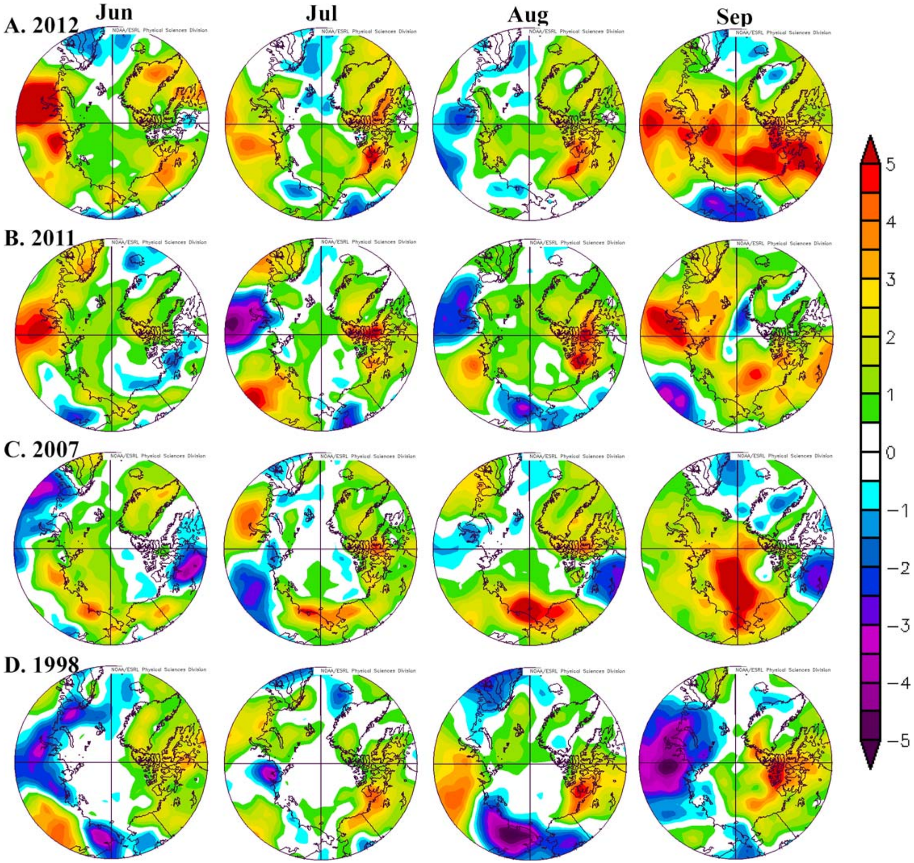

Fig. 8. Spatial distribution of mean June to September surface air temperature (SAT; ˚C) anomalies for 2012, 2011, 2007 and 1998 **(A–D)**. Anomalies calculated with respect to the 1981–2010 climatology.

CC BY

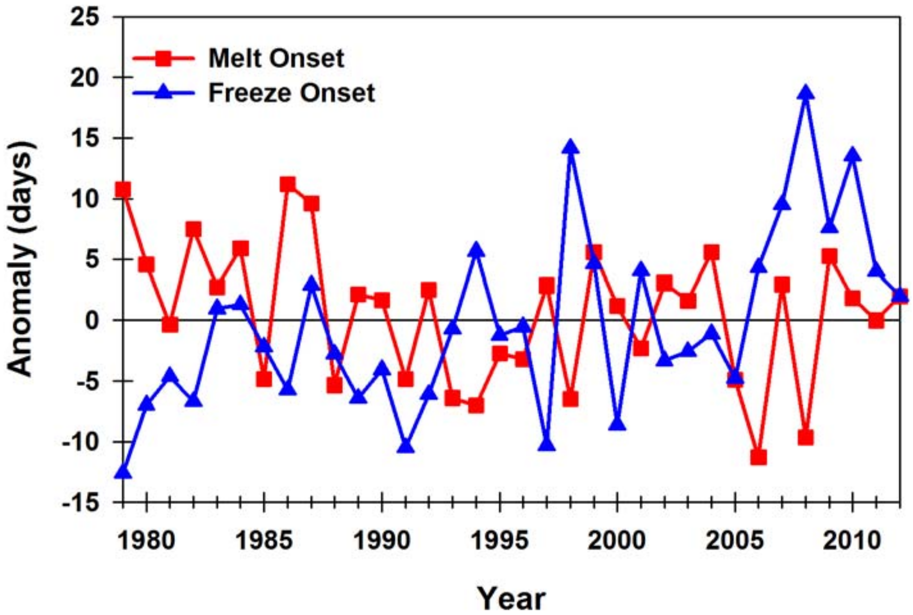

Fig. 9. Time series of the melt and freeze onset anomalies (days) in the Canadian Arctic Archipelago, 1979–2012. Anomalies calculated with respect to the 1981–2010 climatology.

TCD
7, 1313–1358, 2013

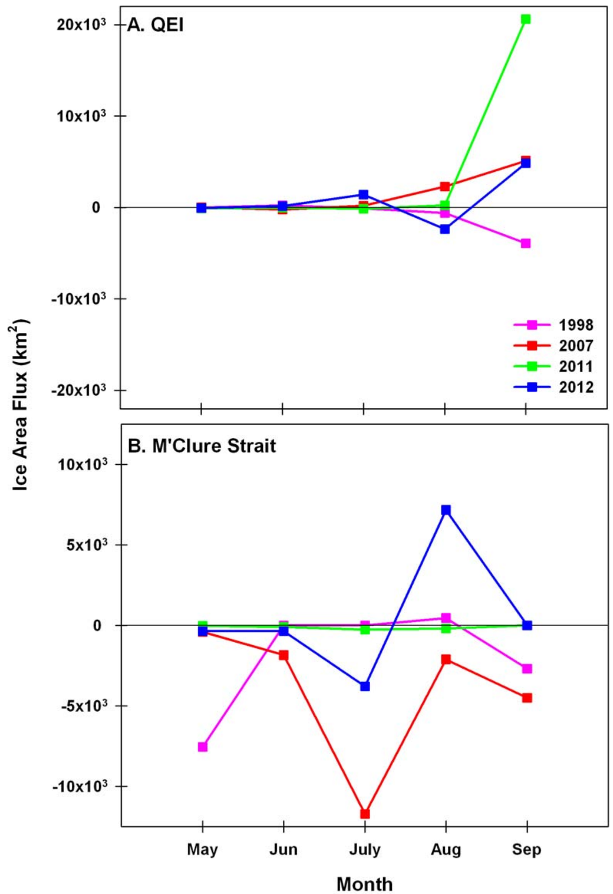

Fig. 10. Time series of mean May to September Arctic Ocean–Canadian Arctic Archipelago sea ice area flux (km^2) at the Queen Elizabeth Islands (QEI) **(A)** and the M'Clure Strait **(B)** for 1998, 2007, 2011 and 2012 estimated from RADARSAT. Positive/negative sign indicates Arctic Ocean inflow/outflow.

CC BY

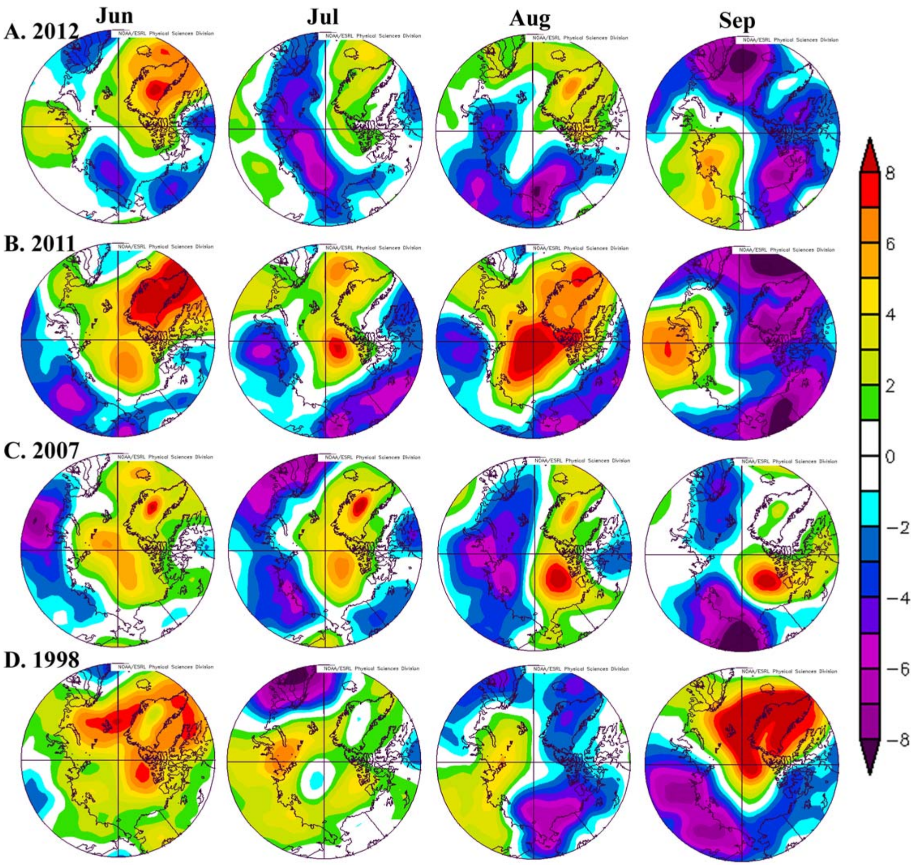

Fig. 11. Spatial distribution of mean June to September sea level pressure (SLP; mb) anomalies for 2012, 2011, 2007 and 1998 **(A–D)**. Anomalies calculated with respect to the 1981–2010 climatology.

TCD
7, 1313–1358, 2013

CC BY

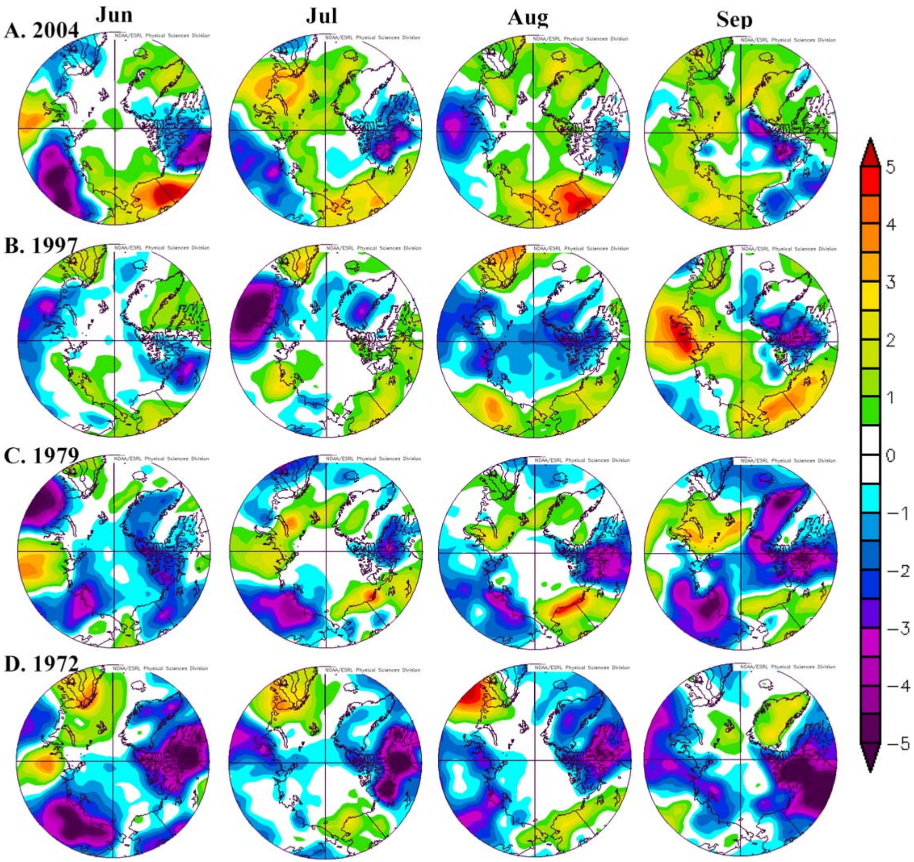

Fig. 12. Spatial distribution of mean June to September surface air temperature (SAT; ˚C) anomalies for 2004, 1997, 1979, and 1972 **(A–D)**. Anomalies calculated with respect to the 1981–2010 climatology.

TCD
7, 1313–1358, 2013
Recent extreme light sea ice years in the Canadian Arctic Archipelago
S. E. L. Howell et al.

cc BY

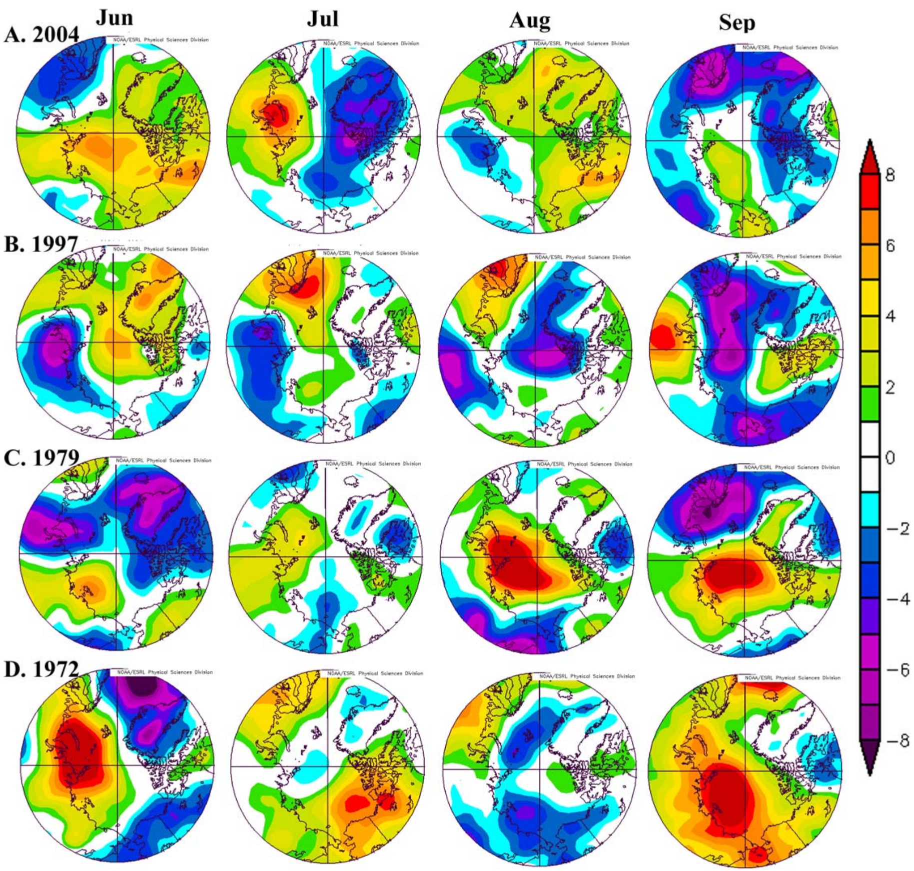

Fig. 13. Spatial distribution of mean June to September (JJAS) sea level pressure (SLP; mbar) anomalies for 2004, 1997, 1979, and 1972 **(A–D)**. Anomalies calculated with respect to the 1981–2010 climatology.

TCD
7, 1313–1358, 2013

cc BY

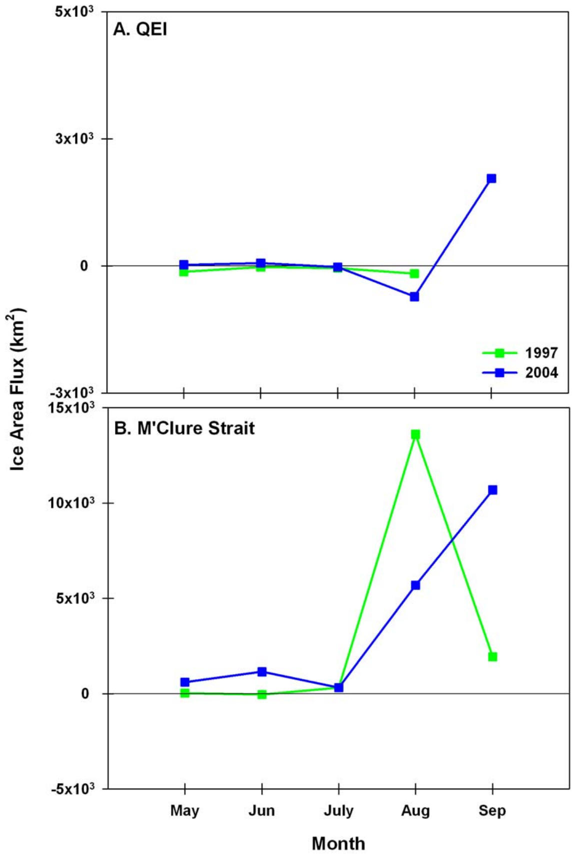

Fig. 14. Time series of mean May to September Arctic Ocean–Canadian Arctic Archipelago sea ice area flux (km^2) at the Queen Elizabeth Islands (QEI) **(A)** and the M'Clure Strait **(B)** for 1997 and 2004 estimated from RADARSAT. No RADARSAT data was available in September 1997 at the QEI. Positive/negative sign indicates Arctic Ocean inflow/outflow.

CC BY

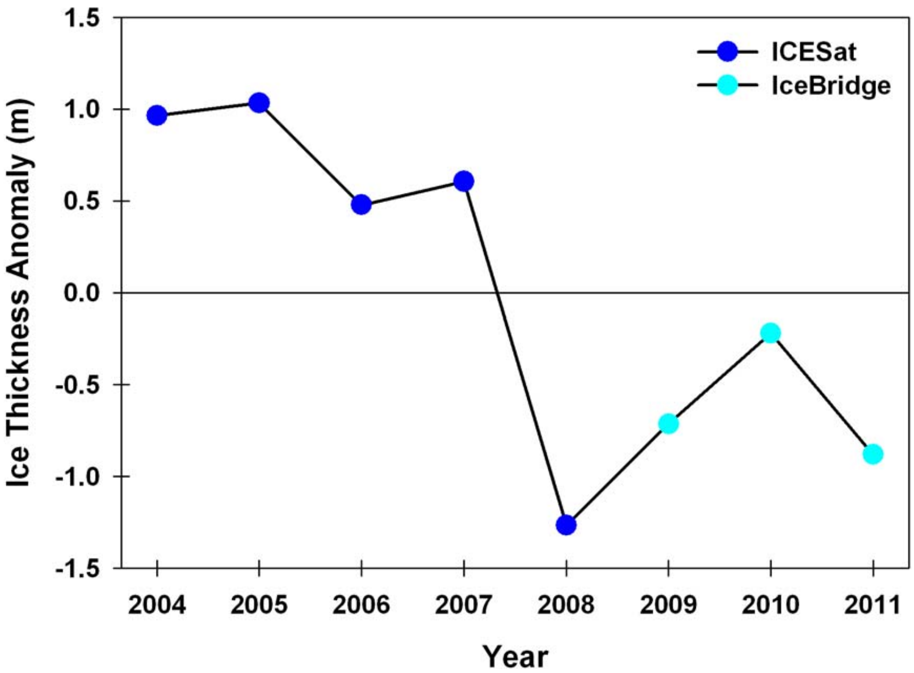

Fig. 15. Time series of ICESat and IceBridge winter Arctic sea ice thickness anomalies in the Canadian Basin just north of the Canadian Arctic Archipelago, 2004–2011. Anomalies are calculated with respect to the 2004–2011 period.

TCD
7, 1313–1358, 2013

CC BY

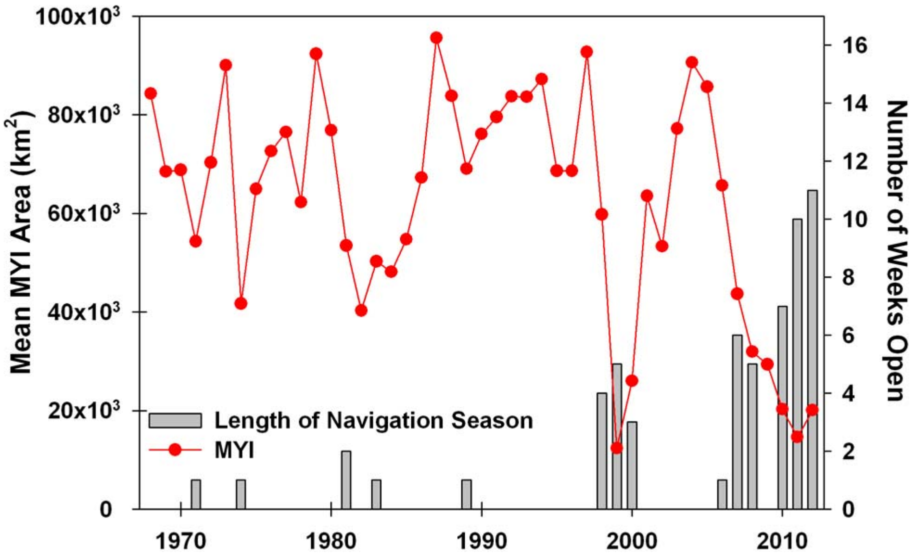

Fig. 16. Time series of the length of the navigation season for the northern route of the Northwest Passage and mean multi-year ice (MYI) area within the region, 1968–2012. The navigation season is defined by the Canadian Ice Service as a 17-week time window from 25 June to 15 October.

TCD
7, 1313–1358, 2013

CC BY